16th European Symposium on Computer Aided Process Engineering
and 9th International Symposium on Process Systems Engineering
W. Marquardt, C. Pantelides (Editors)

Modelling and Simulation of Fe_2O_3/Aluminum Thermite Combustion: Experimental Validation

Luísa Durães,[a] Paulo Brito,[a,b] José Campos,[c] António Portugal[a]

[a]*CEM Group, Chemical Engineering Dept., Faculty of Sciences and Technology, University of Coimbra, Pólo II, Coimbra 3030–290, Portugal*
[b]*Chemical Technology Dept., School of Technology and Management, Bragança Polytechnic Inst., Campus de Santa Apolónia, Bragança 5301–857, Portugal*
[c]*Thermodynamics Group, Mechanical Engineering Dept., Faculty of Sciences and Technology, University of Coimbra, Pólo II, Coimbra 3030–201, Portugal*

Abstract

A one-dimensional model was built to simulate the non-steady radial combustion propagation on thin circular samples of Fe_2O_3/Aluminum thermite mixtures. The model considers zero order kinetics and conductive/radiative heat transfer. All the properties of the system are assumed to vary with the temperature and composition during the propagation and phase transitions are also contemplated. These features, not yet considered in the literature, allowed the obtainment of realistic solutions, readily comparable with experimental values measured in an earlier work. The experimental combustion velocities were used to adjust the kinetic constant of the model, in order to give it a good predictive capability. The predicted combustion temperatures and reaction extents were higher than the experimental. This was justified by the heat losses due to the spraying of products away from the combustion system and the incompleteness of the reaction, observed in experimental conditions and not considered in the model.

Keywords: Combustion, Fe_2O_3/Aluminum thermite, Modelling, Finite differences.

1. Introduction

The self-propagating high temperature reactions, as the Fe_2O_3/Aluminum thermite combustion, are hard to follow by experimentation due to fast chemical and physical transformations and the high temperatures achieved. Hence, many studies concerning theoretical prediction of these combustion processes have been published (Moore and Feng, 1995, Makino, 2001) and represent a valuable guideline for experimental work.

The Fe_2O_3/Aluminum thermite reaction has already been simulated in cylindrical geometry with a one-dimensional coordinate system attached to the uniformly propagating combustion wave (Raymond et al., 1998, Shkadinsky et al., 1997, 2000), and with a fixed one-dimensional coordinate system (Brito et al., 2004). However, the availability of experimental results of radial combustion on disk shaped samples (Durães et al., 2006a) has stimulated, in an earlier work, the derivation of a one-dimensional model to describe the Fe_2O_3/Al radial combustion propagation (Brito et al., 2005). The built model congregates several features of simpler models published (Bowen and Derby, 1995, Carrillo-Heian et al., 1999, Graeve et al., 2001, Cuadrado-Laborde et al., 2003). It considers non-steady propagation with conductive/radiative heat transfer mechanisms and zero order reaction kinetics. Additionally, all the thermophysical properties are assumed to vary with the temperature and composition of the mixture, assumption not yet considered in the literature. Adaptive numerical methods were applied in the resolution, involving a mesh adaptation method based on a

continuous grid refinement technique (Brito, 1998). The solution profiles are fast moving steep fronts, which are validated in this work by experimental results. In the model specifications, the experimental set-up features are considered, namely the reactant samples geometry, dimensions, compositions and density, confinement materials properties and environment conditions. Five thermite mixtures compositions, one stoichiometric and four over aluminized, were experimented and simulated, and the obtained combustion front propagation velocity, temperature and final products composition are compared.

2. Experimental Procedure

Industrial Fe_2O_3 (1.7 μm, 96 %, Bayer) and aluminum (18.6 μm, 89.3 %, Carob) powders were mixed in stoichiometric and over aluminized ratios (vd. Eq. 1 and Table 1). Chemical and physical characterisation of reactants, and mixtures preparation procedure were presented in previous papers (Durães et al., 2006a, 2006b).

$$Fe_2O_3 + 2Al \rightarrow 2Fe + Al_2O_3 \quad (1)$$

Table 1. Thermite mixtures composition.

Mixture	T100	T112	T127	T142	T159
Fe_2O_3:Al molar ratio	1:2	1:2.24	1:2.54	1:2.85	1:3.19
Fe_2O_3:Al mass ratio	1:0.338	1:0.379	1:0.429	1:0.482	1:0.538
Equivalence ratio[a]	1.00	1.12	1.27	1.42	1.59

[a] (O for the oxidation of the existing Al to Al_2O_3)/(O present in the Fe_2O_3 of the mixture).

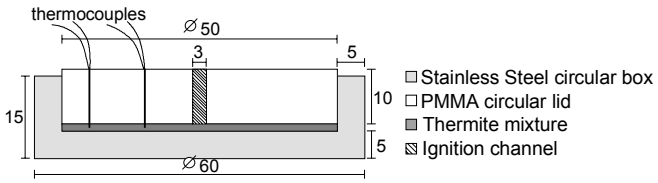

Figure 1. Combustion sample setup (dimensions in mm).

Reactant mixtures were compressed in a stainless steel circular box with an inner PMMA lid (vd. Fig. 1) as described in Durães et al. (2006a). Samples of 1-2 mm thickness were obtained and their porosities varied from 0.30 to 0.50. Samples combustion was initiated in the ignition channel via a nichrome wire instantaneously heated by a capacitor discharge. Radial flame propagation was monitored by digital video-crono-photography. Combustion thermograms were registered at two different radius, using W/Re thermocouples. The obtained radial combustion propagation profiles, rates and temperatures were discussed in Durães et al. (2006a). Finally, the mixtures combustion products were collected and characterized by X-ray diffraction and Mössbauer spectroscopy (Durães et al., 2006b).

3. Model and Numerical Method

The built model is based on the following assumptions: i) one-dimensional radial non-steady propagation; ii) general reaction with mass stoichiometry $\alpha_A A + \alpha_B B \rightarrow \alpha_C C + \alpha_D D$; iii) limiting reactant A; iv) zero order kinetics; v) conductive/radiative heat

transfer mechanisms; vi) negligible relative movement between species; vii) sample dimensions and confinement materials as in Fig. 1. Therefore, the energetic and mass partial balances take the form:

$$\rho_M C_{PM} \frac{\partial T}{\partial t} = \frac{1}{r}\frac{\partial}{\partial r}\left[k_M\left(r\frac{\partial T}{\partial r}\right)\right] + Q\cdot\mathbf{r} - \left[\left(U_{steel/air}+U_{PMMA/air}\right)\left(T-T_0\right)+2\sigma\varepsilon_M\left(T^4-T_0{}^4\right)\right]\Big/Z \quad (2)$$

$$\frac{dW_A}{dt} = -\alpha_A \mathbf{r} \quad (3)$$

σ is the Steffan-Boltzman constant, ε the emissivity, W_A the mass concentration of A, Z the sample thickness and subscript M represents the mixture. The reaction enthalpy ($-Q$) is computed considering the enthalpy variations ($C_P(T)$ integral and phase transitions) at constant pressure of reactants and products in the temperature path $T_0 - T$. The reaction kinetics is defined by $\mathbf{r} = H(T - T_{react})K$, where H is the Heaviside function and K a non-temperature dependent kinetic constant. The last term in Eq. (2) accounts for heat losses through the sample top and bottom to the surrounding (at T_0). The differential problem is completed by the definition of suitable initial and boundary conditions, reformulated in relation to Brito et al. (2005):

$$t = 0 \quad \begin{cases} 0 \le r \le R_0 & \Rightarrow \quad T = T_{igni} \\ r > R_0 & \Rightarrow \quad T = T_0 \end{cases} \quad (4)$$

$$t > 0; \quad r = 0 \quad \Rightarrow \quad \frac{\partial T}{\partial r} = 0 \quad (5)$$

$$t > 0; \quad r = R \quad \Rightarrow \quad k_M \frac{\partial T}{\partial r} = -\left[U'_{steel/air}\left(T-T_0\right)+\sigma\varepsilon_M\left(T^4-T_0{}^4\right)\right] \quad (6)$$

Eq. (4) simulates ignition by a temperature spatial pulse with height T_{igni} and length R_0 at the initial time. On the inner and outer boundaries, a symmetry condition and conductive/radiative heat transfer are considered, respectively.

The thermophysical properties vary with the temperature and composition of the mixture. The mixing rules for each property, with i = A,B,C,D and E (air), are:

$$C_{PM} = \sum_i \omega_i C_{Pi}; \quad \rho_M = 1\Big/\sum_i \frac{\omega_i}{\rho_i}; \quad k_M = \left(1\Big/\sum_i \frac{\upsilon_i}{k_i} + \sum_i \upsilon_i k_i\right)\Big/2; \quad \varepsilon_M = \sum_i \upsilon_i \varepsilon_i \quad (7)$$

where ω_i and υ_i are the mass and volumetric fractions of component i. The mixture conductivity is the average value between the conductivity of a serial and a parallel rearrangement of the components on a very narrow film (thickness Δr) centered on each spatial node position. An equivalent conductivity component is introduced in air conductivity estimative, for the radiation on the void spaces of the serial arrangement ($k'_E = k_E + 4\sigma\varepsilon_M T^3 \upsilon_E \Delta r$). Phase transitions of the components are considered, over a temperature range (ΔT) of 1 K, each time its transition temperatures are crossed, by means of an equivalent C_P: $C'_{Pi} = C_{Pi} + L_i/\Delta T$ (L_i – latent heat).

The model was solved using non-uniform centered finite difference approximations to estimate spatial derivatives and DDASSL numerical integrator to perform time

integration. An adaptive strategy based on successive refinement of an initial one-dimensional uniform spatial grid was developed and described in Brito (1998). Essentially, the adaptive algorithm converts the original problem in a set of subproblems generated by a subgrid selection procedure, in each time step. This selection is done by comparison of the problem solution obtained over a coarse (level 1) and a fine (level 2) grids. The nodes where an error criterion is not verified are grouped in subgrids over which subproblems are generated and solved. The procedure is repeated until the error criterion is verified on all nodes or a maximum refinement level is reached. In the later case, the procedure is repeated with a smaller time step. To avoid numerical problems that could arise due to the definition of boundary conditions for high refinement level subproblems (Brito et al., 2005), in this work it was chosen to only execute temporal step adaptation, fixing the maximum refinement level as 2.

The model solution comprises temperature and composition spatial and temporal profiles. The composition spatial profiles were used to estimate the combustion wave propagation velocity, considering the front position .vs. time. The location of the front was obtained by the 50 % conversion point.

For the particular thermite system under study (Eq. 1), the thermophysical properties of the components and its dependence relations with temperature were given in Brito et al. (2005). Out of the temperature ranges available in the literature, properties values were fixed as the last value known. The confinement materials properties were also defined in Brito et al. (2005). The general data for the simulations are presented in Table 2. It was found that the decreasing of the adaptive algorithm tolerance does not affect significantly the results, only leading to greater execution times.

Table 2. General data for the simulation.

$Q\|_{T_0}$ (J/kg)	T_0 (K)	P (Pa)	T_{igni} (K)	T_{react} (K)	R (m)	R_0 (m)
5322746	298.15	101325	2300	1200	0.025	0.0015
Z (m)	τ (s)[a]	T' (K) [a]	Δr (m)	$\upsilon_{air\ 0}$		
0.0015	0.1	1000	1×10^{-5}	0.392; 0.384; 0.365; 0.370; 0.350[b]		
DDASSL tol.	Algorithm tol.		Finite diff. points	1st and 2nd level grid nodes		
1×10^{-6}	1×10^{-2}		5	41; 81		

[a] Time and temperature normalization constants;
[b] Experimental mean porosity for T100, T112, T127, T142 and T159, respectively.

4. Discussion of Results and Conclusions

As expected, the temperature and composition spatial and temporal profiles are steep propagation waves. They are aproximatelly constant velocity waves with constant maximum temperature, except in the boundary regions. The conversion was complete in all cases. There was a minimum kinetic constant (K) value for self-propagation of the combustion wave: 7000 kg/(m^3.s) for T100 and T112, 8000 kg/(m^3.s) for T127 and T142, and 9000 kg/(m^3.s) for T159. Figure 2 exemplifies the obtained profiles with minimum K. During the radial propagation, the front velocity tended to a constant value (vd. Fig. 3). These steady values are presented in Fig. 4 as function of K. The mean maximum temperature values, for $0.5 \leq (r/R) \leq 0.8$, are also included. For each mixture, the increasing of K led to higher mean maximum temperatures and wave propagation velocities, as expected. The excess of aluminum in the mixtures improved the heat transfer in the system, by the increase of the thermal conductivity, and enhanced the

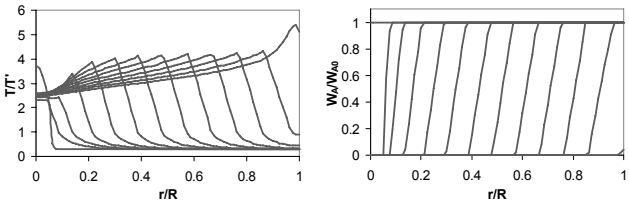

Figure 2. Temperature and composition radial profiles for the T100 combustion with minimum *K*. Time gap between profiles - 0.3 s.

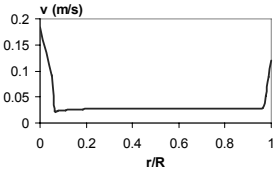

Figure 3. Typical combustion front velocity .vs. radius. Case of T100 mixture with *K*=100000 kg/(m^3.s).

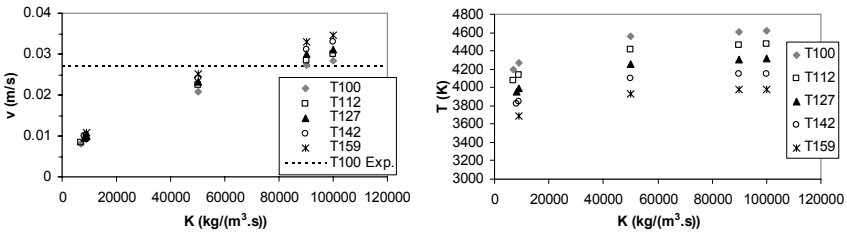

Figure 4. Combustion front velocities and mean maximum temperatures with several *K* values.

combustion propagation velocity. However, as the aluminum excess represents an additional thermal capacitance without contributing to an increase of heat released by the reaction, a higher aluminum excess led to lower mean maximum temperatures.

Considering the stoichiometric mixture as a reference, an optimum *K* value was selected – 90000 kg/(m^3.s) – to adjust the predicted combustion front velocity to the experimental value (vd. Fig. 4). Figure 5 presents the temperature profiles for T100 and T159 combustion with the selected *K*. The other mixtures led to intermediate profiles. Higher values of *K* led to steeper and more uniform profiles (vd. Figs. 2 and 5). The same was verified for the composition profiles. The calculated combustion front velocities, with selected *K* and for all mixtures, are given in Fig. 6 and compared with experimental results. A good agreement for T100 and T112 mixtures was reached. For the other mixtures, the predicted values are considerably lower than the experimental. This discrepancy is due to the experimental occurrence of a consecutive exothermic intermetallic reaction, which formed Fe_3Al when aluminum was in excess and enhanced the front velocity (Durães et al., 2006a, 2006b). This reaction was not considered in the model. Experimentally, a nearly stoichiometric condition was only achieved between T112 and T127 mixtures, due to the incompleteness of reaction (Durães et al., 2006b). The model always gave complete conversion. The predicted combustion temperatures

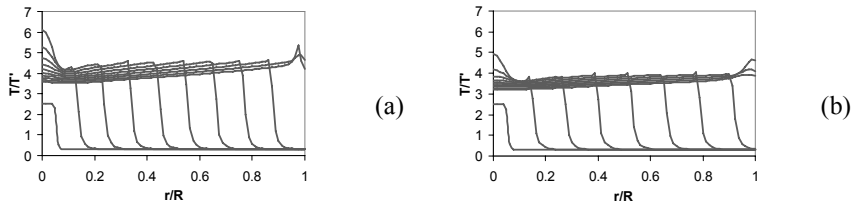

Figure 5. Temperature profiles obtained in the radial combustion of (a) T100 and (b) T159 mixtures with *K*=90000 kg/(m^3.s). Time gap between profiles - 0.1 s.

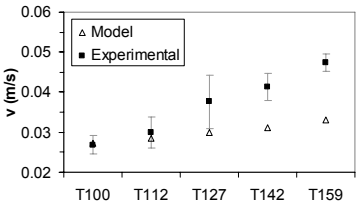

Figure 6. Experimental and predicted (K=90000 kg/(m^3.s)) combustion front velocities.

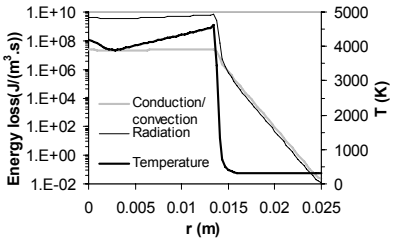

Figure 7. Temperature and heat losses radial profiles obtained for T100 mixture, with 90000 kg/(m^3.s) and t=0.5 s.

were higher than the experimental mean value (≈ 2300 K). This is justified by the heat losses due to the spraying of products away from the combustion system, observed experimentally and not considered in the model.

Figure 7 presents the typical heat losses radial profiles calculated for a median time of the propagation. The radiative term is ≈ 100 times higher than the condutive/convective term in the combustion products region, where the temperature is very high. In the reactants region, the magnitude of these terms is comparable and strongly decreases.

References

C.R. Bowen and B. Derby, 1995, Finite-difference modelling of self-propagating high-temperature synthesis of materials, Acta Metall. Mater., 43(10), 3903.

P. Brito, 1998, Aplicação de métodos numéricos adaptativos na integração de sistemas algébrico-diferenciais caracterizados por frentes abruptas, MSc. Thesis, University of Coimbra.

P. Brito, L. Durães, J. Campos and A. Portugal, 2004, Aplicação de métodos adaptativos para a simulação de processos de combustão, in: Proc. of CMCE 2004, APMTAC & SEMNI & LNEC, Lisboa, p. 472 & CD-ROM.

P. Brito, L. Durães, J. Campos, A. Portugal, 2005, Modelling and simulation of Fe_2O_3/Al thermite combustion in: Proc. of CHEMPOR 2005, Chem. Eng. Dept., Coimbra, p. 157 & CD-ROM.

E.M. Carrillo-Heian, O.A. Graeve, A. Feng, J.A. Faghih and Z.A. Munir, 1999, Modeling studies of the effect of thermal and electrical conductivities and relative density of field-activated self-propagating combustion synthesis, J. Mater. Res., 14(5), 1949.

C. Cuadrado-Laborde, L.C. Damonte and L. Mendoza-Zélis, 2003, Theoretical treatment of a self-sustained, ball milling induced, mechanochemical reaction in the Fe_2O_3-Al system, Mater. Sci. Eng., A355, 106.

L. Durães, J. Campos and A. Portugal, 2006a, Radial combustion propagation in iron(III) oxide/ aluminum thermite mixtures, Propell. Explos. Pyrot., 31(1), 42.

L. Durães, B. Costa, R. Santos, A. Correia, J. Campos and A. Portugal, 2006b, Fe_2O_3/Aluminum thermite reaction intermediate and final products identification, Comb. Flame. Submitted.

O. Graeve, E. Carrillo-Heian, A. Feng and Z. Munir, 2001, Modeling of wave configuration during electrically ignited combustion synthesis, J. Mater. Res., 16(1), 93.

J.J. Moore and H.J. Feng, 1995, Combustion synthesis of advanced materials: Part II. Classification, applications and modelling, Prog. Mater. Sci., 39, 275.

A. Makino, 2001, Fundamental aspects of the heterogeneous flame in the self-propagating high-temperature synthesis (SHS) process, Prog. Energy Comb. Sci., 27, 1.

C.S. Raymond, K.G. Shkadinsky and V.A. Volpert, 1998, Gravitational effects on liquid flame thermite systems, Comb. Sci. Technol., 131, 107.

K. Shkadinsky, G. Shkadinskaya and B. Matkowski, 2000, Gas-phase influence on quasisteady "liquid flames" in gravitational fields, Comb. Sci. Technol., 157, 87.

K. Shkadinsky, G. Shkadinskaya and V. Volpert, 1997, Stability of "liquid flame" combustion waves Chem. Eng. Sci., 52(9), 1415.